Published in final edited form as:
J Infect Dis. 2010 November 1; 202(9): 1397–1404. doi:10.1086/656524.

The stringent response is required for full virulence of *Mycobacterium tuberculosis* in guinea pigs

Lee G. Klinkenberg[1], **Jong-Hee Lee**[1], **William R. Bishai**[1,2], and **Petros C. Karakousis**[1,2,*]

[1] Center for Tuberculosis Research, Department of Medicine, Johns Hopkins University School of Medicine, Baltimore, USA

[2] Department of International Health, Johns Hopkins Bloomberg School of Public Health, Baltimore, USA

Abstract

During human latent tuberculosis (TB) infection, *Mycobacterium tuberculosis* likely resides within the nutrient-starved environment of caseous lung granulomas. The stringent response alarmone (p)ppGpp is synthesized by Rel in response to nutrient starvation, thus enabling tubercle bacilli to restrict growth and shut down metabolism in a coordinated fashion. In this study, we investigated the virulence of a *rel*-deficient *M. tuberculosis* mutant in the guinea pig model. Quantitative RT-PCR was used to study the effect of (p)ppGpp deficiency on expression of key cytokine and chemokine genes in guinea pig lungs. The *rel*-deficient mutant showed impaired initial growth and survival relative to the wild-type strain. Loss of Rel was associated with the striking absence of tubercle lesions grossly and of caseous granulomas histologically. The attenuated phenotype of the *rel*-deficient mutant was not associated with increased expression of genes encoding the proinflammatory cytokines IFN-γ and TNF-α in the lungs 28 days after infection.

Keywords

Mycobacterium tuberculosis; stringent response; Rel; virulence; persistence; latency; granuloma; alarmone; (p)ppGpp; guinea pig; animal models

Introduction

One of the major challenges facing global TB eradication efforts is the fact that two billion people are latently infected with *M. tuberculosis*, many of whom, especially in the setting of HIV co-infection, will eventually develop disease. Soon after their inhalation, tubercle bacilli are engulfed by alveolar macrophages, leading to potent cell-mediated immune responses and granuloma formation [1,2]. Within eight weeks after infection and coincident with the development of delayed-type hypersensitivity (DTH), these granulomas undergo caseous necrosis, resulting in the destruction of surrounding host tissue and bacillary death [3]. Latent TB infection, defined as tuberculin skin test reactivity without any clinical or radiographic findings, is thought to comprise the surviving paucibacillary population of nonreplicating and slowly metabolizing organisms [4], which have adapted to the unfavorable milieu within

* Corresponding author: Petros C. Karakousis, Center for Tuberculosis Research, Johns Hopkins University School of Medicine, 1550 Orleans Street, Room 106, Baltimore, MD 21231-1001, 410-502-8233, Fax: 410-614-8173, petros@jhmi.edu.

The authors of this manuscript have no conflicts of interest to report.

Portions of this work were presented at: 2009 Keystone Symposium on Tuberculosis (poster number 282); 45th annual meeting of IDSA (oral presentation); 46th annual meeting of IDSA (poster number 1081)

caseating granulomas [5]. The microenvironment encountered by these dormant bacilli in human TB lesions likely includes hypoxia [6], as well as nutrient limitation and acidic pH [7]. Subsequent reactivation of infection is thought to result from dampening of host immune responses.

In many microorganisms, including *M. tuberculosis*, the stress of nutrient depletion leads to a dramatically slowed growth state characterized by decreased rRNA, tRNA, and protein synthesis, modified RNA polymerase activities, diminished activity of many transport systems and decreased carbohydrate, amino acid, and phospholipid metabolism. This so-called stringent response is in part mediated by the rapid intracellular accumulation of hyperphosphorylated guanosine nucleotides, including the 3′-pyrophosphate derivative of GDP (ppGpp) and GTP (pppGpp), the mixture being referred to as (p)ppGpp [8]. The alarmone (p)ppGpp interacts with RNA polymerase [9,10], thus altering sigma factor competition for RNA polymerase and modulating promoter recognition and activity [11,12]. In Gram-negative bacteria, two separate enzymes, RelA and SpoT, are primarily responsible for the synthesis and hydrolysis, respectively, of (p)ppGpp [13]. In *M. tuberculosis*, the dual-function enzyme Rel catalyzes both ATP:GTP 3′-pyrophosphoryltransfer and (p)ppGpp 3′-pyrophosphohydrolysis [14,15]. When uncharged tRNA occupies the acceptor site of a ribosome stalled at a codon on an mRNA, the ribosome-bound Rel is stimulated to synthesize (p)ppGpp, signaling a limitation in amino acids. Conversely, when amino acid levels are sufficient, (p)ppGpp is hydrolytically degraded by Rel [15].

The ability to fine-tune cellular (p)ppGpp concentrations through Rel in response to available nutrients or other stresses is essential for the long-term survival of *M. tuberculosis* under growth-limiting conditions. Thus, inactivation of the gene Rv2583c encoding Rel yielded a strain H37Rv Δ*rel* unable to synthesize (p)ppGpp and defective in long-term survival upon nutrient starvation [8] and extended anaerobic incubation in vitro [8], as well as during the chronic phase of infection in mouse lungs [16]. Similarly, a *rel*-deficient mutant showed impaired survival in a mouse granuloma model of latent TB infection [17]. However, a major deficiency of murine TB models is that mouse lesions lack caseation necrosis, which is the pathological hallmark of human TB granulomas [18,19], where dormant bacilli are believed to reside during latent TB infection [5,20]. On the other hand, guinea pig TB granulomas more closely approximate their human counterparts with respect to cellular composition, granuloma architecture, and the presence of caseation necrosis [18]. In addition, tissue hypoxia is present in guinea pig TB granulomas [21,22], but absent in mouse TB lung lesions [21,23,24]. To investigate the role of the *M. tuberculosis* stringent response in bacillary survival and TB-related pathology in a highly relevant animal model, we studied the behavior of a *rel*-deficient mutant in the guinea pig model of TB infection. We also determined the effect of loss of Rel on lung cytokine gene expression.

Materials and Methods

Bacterial strains, media, and growth conditions

A *M. tuberculosis* H37Rv strain deficient in Rv2583c/*rel* (Δ*rel*) and the isogenic wild-type strain [8] were kindly provided by Dr. Valerie Mizrahi. Each strain (including *rel* Comp, see below) was twice-passaged through the guinea pig and grown to mid-logarithmic phase (OD_{600} ~0.8) at 37°C in supplemented Middlebrook 7H9 liquid broth (Difco).

Construction of a rel-complemented strain

M. tuberculosis H37Rv genomic DNA was purified as previously described [25] and the *M. tuberculosis rel* open reading frame was PRC-amplified using forward primer 5′-GGCCTCTAGAGACGAAAATGTATGCGGTGA-3′and reverse primer 5′-

GGCCTCTAGACTACGCGGCCGAGGTCACCCGGTA-3′, which introduce *Xba*I restriction sites at the 5′ and 3′ ends of the amplicon. This PCR product includes the entire coding sequence of *rel* and the upstream gene *apt*, as well as the native promoter sequence [8,26]. The *Xba*I-digested fragment was inserted into the integrative plasmid pMH94 [27], and the ensuing plasmid pRelMtb Comp, was electroporated into Δ*rel* [28], generating the *rel*-complemented strain (*rel* Comp) (Fig. 1a).

Guinea pigs

Female Hartley guinea pigs (250-300g, Charles River) were housed in a Biosafety Level-3 (BSL-3), pathogen-free animal facility and were fed water and chow *ad libitum*. The animals were maintained and all procedures performed according to protocols approved by the Institutional Animal Care and Use Committee at the Johns Hopkins University School of Medicine.

Infection of animals and virulence endpoints

Separate groups of guinea pigs were aerosol-infected with wild-type *M. tuberculosis* H37Rv, Δ*rel*, or *rel* Comp using an inhalation exposure system (Glas-col) calibrated to deliver ~100 bacilli per animal. Four guinea pigs from each group were sacrificed on Days 1, 14, 28, and 56, after infection.

At the designated time points, lungs and spleens from sacrificed animals were removed aseptically, weighed, and examined. Organs were then homogenized for colony-forming unit (CFU) enumeration and processed for histology. Lungs were homogenized in 10-15 ml PBS using a Kinematica Polytron Homogenizer with a 12-mm generator (Brinkman) within a BSL-III Glovebox Cabinet (Germfree). Spleens were homogenized in 1-ml PBS using glass homogenizers. Serial tenfold dilutions of organ homogenates were plated on 7H11 selective agar (BBL) except for Day 1 lung samples, which were plated neat. Plates were incubated at 37°C and CFU were counted after 4 weeks.

At various time points after infection, lung samples were fixed in 10% PBS-buffered formalin, paraffin-embedded, and sectioned. Sections were stained with hematoxylin/eosin and Ziehl–Neelsen for microscopy.

For DTH responses, guinea pigs in the 5^{th} week of infection were shaved and injected intradermally with 50 tuberculin units of H37Rv purified-protein derivative. The largest diameter of skin induration was recorded after 24 hours.

Host lung gene expression analysis

Guinea pigs were aerosol-infected with ~50 bacilli of wild type or Δ*rel* per animal lung. On Day 1 and Day 28 after infection, lungs were rapidly homogenized, as described above, in TRIzol reagent (Invitrogen) and frozen. Each lung sample (1-ml homogenate) was subjected to 8 pulses of bead beating (30 s/pulse) separated by 1 min on ice, and nucleotides were extracted according to the manufacturer's protocol (Invitrogen). RNA was purified using the RNeasy protocol (Qiagen) and DNA contaminants were removed using two rounds of Turbo DNA-Free (Applied Biosystems).

First strand cDNA synthesis was performed as per Superscript III (Invitrogen) protocols using 0.875 μg prepared RNA, Oligo(dT)15 primer (Promega), and RNAse Out (Invitrogen). Negative controls were prepared for each sample using identical procedures without Superscript III. Gene expression levels of specific cytokines and chemokines were measured using previously published primers [29-32] and an iCycler 5.0 (Bio-RAD). The cycle threshold value (C_T) obtained for each gene was normalized with that of the house-keeping gene encoding

HPRT (hypoxanthine-guanine phosphoribosyltransferase) [30] at each time point in each group. The normalized C_T at Day 28 was then subtracted from the normalized C_T at Day 1 in the same group to yield the normalized ΔC_T for each particular group.

Statistical analysis

The mean of log-transformed lung CFU values, based on four samples for each measure, were compared by the Student *t*-test. A *p*-value of < .05 was considered statistically significant. Statistical analysis of gene expression studies was performed using three biological replicates of each sample at each time point. Synthesized cDNA was subjected to three technical replicates of PCR amplification for each biological sample. Each individual reaction was compared to a reaction lacking reverse transcriptase (background signal). Melt curves were generated for each reaction and successful reactions contained only one melt peak above threshold, representing a single amplicon per reaction. Normalized technical replicate values were averaged to generate a single value for each biological sample. Mean and standard deviation (SD) were then calculated for the three biological replicate values of each gene of interest.

Results

Construction and genotypic characterization of a rel-complemented strain

The *rel* (Rv2583c) gene was deleted previously from *M. tuberculosis* H37Rv by allelic exchange, generating Δ*rel* [8]. In order to confirm that the mutant phenotype was attributable to *rel* deficiency, a *rel*-complemented strain (*rel* Comp) was constructed (Fig. 1a). PCR amplification of a region of *rel* revealed a product of the correct size in wild-type and *rel* Comp strains, which was absent in Δ*rel* (Fig. 1b). The *rel* Comp strain can be distinguished genetically from wild-type strain by the presence of a hygromycin-resistance cassette, which is also present in Δ*rel*, and by the presence of a unique kanamycin-resistance cassette (Fig. 1b). Single-copy integration of *rel* at the proper location is expected to produce a 4.6-kb restriction fragment compared to a 10-kb restriction fragment in the wild type following digestion with *Bam*HI (Fig. 1c). These findings were further corroborated by Southern blot (Fig. 1d) using a DNA probe recognizing the region shown in Fig. 1c.

The stringent response is required for optimal initial growth and survival of M. tuberculosis in guinea pig lungs

Guinea pigs were aerosol-infected with wild type, Δ*rel*, or *rel* Comp. During the first 14 days after infection, wild-type and *rel* Comp strains showed typical exponential growth, reaching a peak lung burden of 5.15 ± 0.29 $\log_{10}$ and 4.92 ± 0.35 $\log_{10}$, respectively (Fig. 2). Δ*rel* showed a mild but statistically significant initial growth defect relative to wild type, increasing to only 4.57 $\log_{10} \pm 0.05$ (p=.007). After the onset of adaptive immunity, the wild type maintained a stable lung census at Days 28 and 56. Although the lung CFU of Δ*rel*-infected animals declined slightly to 4.35 ± 0.38 $\log_{10}$ at Day 28 (p=.28), they decreased dramatically to 2.09 ± 0.46 $\log_{10}$ (p< .00004) at Day 56. The *rel* Comp strain mostly restored the wild-type survival phenotype and the CFU of the *rel* Comp strain at Day 56 was not statistically significantly different from that of wild type.

Rel deficiency is associated with reduced gross pathology and histopathology in guinea pig lungs

All guinea pigs survived throughout the duration of the experiment and gained weight equivalently (Table 1). Guinea pig lung weights in wild-type and *rel* Comp groups were 5.13 ± 0.38 g and 4.47 ± 0.27 g, respectively, on Day 28 and 5.26 ± 0.21 g and 5.06 ± 0.43 g, respectively, on Day 56. In contrast, lung weights of Δ*rel*-infected animals were only $3.84 \pm$

0.25 g on Day 28 (p=.029) and 4.22 ± 0.81 g on Day 56 (p=.046) (Table 1). Gross examination of lungs infected with wild-type and *rel* Comp strains on Day 56 revealed discrete tubercle lesions distributed throughout the lung surface (Fig. 3a and 3c, respectively), while Δ*rel*-infected lungs revealed minimal inflammation without discrete lesions.

Histological examination of Day 56 guinea pig samples infected with wild-type and *rel* Comp strains revealed significant lung involvement, with areas of peribronchiolar inflammation and multiple well-circumscribed granulomas comprising primarily lymphocytes and histiocytes with central necrosis (Fig. 3d and 3f, respectively). Ziehl-Neelsen staining revealed the presence of multiple acid-fast bacilli in the periphery of granulomas (Fig. 3d inset and 3f inset). In contrast, histological evaluation of Δ*rel*-infected lung samples revealed significantly reduced inflammation overall, and, despite examination of multiple lung sections, the absence of granulomas (Fig. 3e). In addition, acid-fast bacilli could not be identified in these lung samples.

Animals infected with Δ*rel* mounted smaller DTH responses (7.3 ± 4.0 mm) relative to those infected with wild type (11.0 ± 2.6 mm) and Δ*rel* Comp (9.0 ± 3.0 mm), but these results did not reach statistical significance.

Loss of Rel is associated with reduced dissemination to the spleen

CFU counts in the spleens paralleled those in the lungs. At Day 28 the spleen CFU were 3.53 ± 0.80 $\log_{10}$ and 3.47 ± 1.23 $\log_{10}$ in wild-type and *rel* Comp groups, respectively, while those of Δ*rel*-infected animals were only 2.75 ± 0.82 $\log_{10}$ (p=.23) (Table 1). The trend of lower CFU in the mutant group persisted at Day 56 as spleen CFU values were 2.1 ± 1.28 $\log_{10}$ and 2.98 ± 0.71 $\log_{10}$ in wild-type and *rel* Comp groups, respectively, and 1.56 ± 1.02 $\log_{10}$ (p=.53). Spleen CFU counts were lower than expected in all groups [33].

Guinea pig spleen weights followed the same trend as lung weights. Thus, spleen weights in wild-type and *rel* Comp groups increased from 313 ± 76 mg and 470 ± 158 mg, respectively, on Day 1 to 1233 ± 217 mg and 1110 ± 245 mg, respectively, on Day 28, and remained elevated at 873 ± 84 mg and 955 ± 145 mg, respectively, on Day 56. In contrast, spleen weights of Δ*rel*-infected animal increased from 420 ± 134 mg on Day 1 to a maximal value of 895 ± 159 mg on Day 28 (p=.046) and 648 ± 161 mg on Day 56 (p=.048) (Table 1).

Reduced virulence of the rel-deficient mutant is not associated with increased expression of proinflammatory cytokine genes in guinea pig lungs

Global gene expression studies revealed that *rel* deficiency resulted in differential expression of several genes encoding important *M. tuberculosis* antigens [34]. We hypothesized that altered expression of these antigens in Δ*rel* may enhance expression of proinflammatory cytokines in guinea pig lungs, resulting in increased killing of the mutant strain relative to wild-type. RNA was harvested from lungs infected with the Δ*rel* and wild-type strains of Day 1 and Day 28 after infection. As shown in Figure 4, the relative expression of genes encoding IL-8, TGF-β, and MCP-1 did not differ in the lungs infected with Δ*rel* or wild-type on Day 28 after infection. However, mRNA transcripts of the proinflammatory cytokines IFN-γ, IL-1B, and TNF-α were less abundant in Δ*rel*-infected lungs by 2.2 ± 0.7 cycles (p=.06), 0.8 ± 0.6 cycles (p=.20), and 1.8 ± 0.1 cycles (p=.003), respectively, relative to the corresponding transcripts in wild-type-infected lungs on Day 28.

Discussion

The stringent response is a transcriptional program required for coordinated metabolic shutdown and long-term survival of *M. tuberculosis* under conditions restricting bacillary

growth [8,34]. Inability to mount this adaptive response may result in a futile attempt at continued bacillary growth and metabolism in the face of adverse conditions, ultimately leading to impaired long-term survival of *M. tuberculosis*. In this study, we show that Rel is required for full *M. tuberculosis* virulence in the guinea pig model, as measured by lung and spleen CFU counts, lung and spleen weights, DTH, and lung gross pathology and histology. Importantly, we found that deficiency of Rel is associated with markedly reduced survival in guinea pig lungs. This survival defect became readily apparent by Day 56 after guinea pig infection, much earlier than its appearance in the mouse model of chronic TB infection [34]. Our findings are consistent with the accelerated detection of survival defects of other *M. tuberculosis* mutant strains in guinea pigs relative to mice [35,36].

Incomplete restoration of wild-type CFU counts in guinea pig lungs by *rel* Comp may be explained by the presence of a second copy of the upstream gene *apt* in the putative operon or high levels of expression of the hygromycin-resistance gene, which might lead to a loss of fitness, and/or changes in *rel* expression caused by localization to the attB region of the *M. tuberculosis* genome. However, *rel* Comp successfully matched the wild-type phenotype in all other virulence parameters assessed.

One of the major findings of the current study is the lack of classical TB-related pathology in the lungs of guinea pigs infected with Δ*rel*, which was associated with mildly diminished DTH responses. In addition to playing an important role in slowing *M. tuberculosis* metabolism during the stringent response, intracellular (p)ppGpp levels may also control expression of key virulence genes [34]. Transcriptional analysis of the Δ*rel* mutant by Dahl et al. revealed the Rel-dependent expression of several polyketide synthases, whose products are involved in modulating the host immune response. In addition, Rel may regulate the expression of several genes encoding members of the PE/PPE/PE-PGRS proteins, which are cell surface constituents thought to play a role in antigenic variation and host-pathogen interactions[37]. In particular, the Δ*rel* mutant showed altered expression of eight genes encoding PE/PPE/PE-PGRS proteins thought to play a role in granuloma formation and persistence [38]. Reduced expression of one or more of these proteins may partially explain the absence of granuloma formation in the lungs of Δ*rel*-infected guinea pigs in our study. Our finding of less abundant TNF-α mRNA transcripts in the lungs of mutant –infected animals correlates with the known role of TNF-α in macrophage activation and granuloma formation in the guinea pig TB model [39].

Genes encoding components of the antigen 85 (Ag85) complex, including Rv1886c (*fbpB*; Ag85B), Rv3803 (*fbpD*; Ag85D), and Rv3804c (*fbpA*; Ag85A) were shown to be overexpressed in Δ*rel* relative to wild type [34], suggesting that expression of these genes is negatively regulated by (p)ppGpp. The Ag85 complex induces potent T-cell proliferation responses and IFN-γ production in most *M. tuberculosis*-infected individuals and in BCG-vaccinated mice and humans [40,41]. Expression of Rv3763c (*lpqH*) encoding the 19-kilodalton lipoprotein appears to be positively regulated by Rel [34]. This 19-kDa protein is a major T cell antigen, which has been shown to inhibit secretion of proinflammatory cytokines, including IL-12 and TNF-α, and decrease antigen presentation by macrophages [42]. Contrary to the hypothesis that enhanced clearance of Δ*rel* in animal lungs may be attributable to greater Th1 responses resulting from increased host recognition of Ag85 and/or reduced secretion of the 19-kDa antigen [34], we found that expression levels of genes encoding IFN-γ and TNF-α were lower in the lungs of Δ*rel*-infected animals soon after the onset of adaptive immunity.

There are several potential interpretations of our gene expression findings. First, in our study, we measured host cytokine gene expression levels, which may not accurately reflect protein expression levels. Furthermore, a single time point was used to study the host immune response, chosen to coincide with the establishment of cell-mediated immune responses, which are apparent in guinea pigs by 3-4 weeks after infection [19]. It is possible, for example, that

increased expression of genes encoding IFN-γ and TNF-α in mutant-infected lungs preceded our measurement, and higher levels of these cytokines caused killing of Δ*rel*, returning to baseline values by Day 28 after infection. Contrary to this hypothesis, the survival defect of Δ*rel* in the lungs of guinea pigs became most apparent during the chronic phase of infection between Day 28 and Day 56 after infection. Alternatively, reduced expression of proinflammatory cytokine genes in mutant-infected lungs may be attributable to downregulation of genes encoding various secreted antigens in the mutant, including the potent T cell antigen ESAT-6 [34]. It is interesting to note that *M. bovis* deficient in the *esat6* gene was found to have reduced virulence in guinea pigs, as measured by mycobacterial culture of tissues, gross pathology, and histopathology [43]. Finally, the lower CFU counts (and, consequently, lower overall antigen burden) in Δ*rel*-infected animals, which were apparent by Day 14 after infection, may account for the reduced host immune responses vis-à-vis host cytokine gene expression, gross pathology, histopathology, and DTH.

In a recent study, Ly et al. measured cytokine mRNA profiles of primary and secondary granulomas of *M. bovis* BCG-vaccinated and unvaccinated guinea pigs challenged with virulent *M. tuberculosis* using laser capture microdissection (LCM) of TB lesions [44]. These authors found that primary lesions from unimmunized animals, closely reflecting the conditions in our study, were dominated by TNF-α mRNA. The use of whole lung homogenates rather than LCM in our study may have resulted in failure to accurately detect host TNF-α and IFN-γ mRNA levels within TB lesions. However, the use of LCM in our study was precluded by the lack of discernable tubercle lesions in mutant-infected lungs. We believe that our analysis using the ratio of cytokine gene expression between groups is valid, since lung samples from each infected group were handled in the same manner. Finally, use of whole lung homogenates would be expected to dampen any cytokine mRNA signal because of the inclusion of grossly “normal” lung tissue. Therefore, we would expect that our host gene expression results would be simply magnified by using tissue from discrete histological lesions.

In conclusion, we have demonstrated that the stringent response is critical for optimal virulence of *M. tuberculosis* in guinea pigs. We did not find any evidence that enhanced clearance of Δ*rel* in guinea pig tissues is associated with the induction of more robust host immune responses. On the contrary, loss of Rel led to relatively lower induction of proinflammatory cytokine genes in the lungs, mildly attenuated DTH responses, and the striking absence of caseous granulomas and tubercle lesions. It remains to be demonstrated whether small molecule inhibitors of Rel could be used to target persistent bacilli, thereby shortening the duration of TB chemotherapy.

Acknowledgments

This work was supported by NIH grants: AI064229 and AI083125 to PCK; Potts Memorial Foundation fellowship to LGK.

References

1. Flynn JL, Chan J. Tuberculosis: latency and reactivation. Infect Immun 2001;69:4195–201. [PubMed: 11401954]
2. Kaplan G, Post FA, Moreira AL, et al. Mycobacterium tuberculosis growth at the cavity surface: a microenvironment with failed immunity. Infect Immun 2003;71:7099–108. [PubMed: 14638800]
3. Grosset J. Mycobacterium tuberculosis in the extracellular compartment: an underestimated adversary. Antimicrob Agents Chemother 2003;47:833–6. [PubMed: 12604509]
4. Nuermberger E, Bishai WR, Grosset JH. Latent tuberculosis infection. Semin Respir Crit Care Med 2004;25:317–36. [PubMed: 16088473]
5. Opie ELAJ. Tubercle bacilli in latent tuberculous lesions and in lung tissue without tuberculous lesions. Arch Pathol Lab Med 1927;4:1–21.

6. Haapanen JH, Kass I, Gensini G, Middlebrook G. Studies on the gaseous content of tuberculous cavities. Am Rev Respir Dis 1959;80:1–5. [PubMed: 13670382]
7. Gomez, J.; McKinney, J. Persistence and drug tolerance. In: Rom, W.; Garay, S., editors. Tuberculosis. 2nd. Philadelphia: Lippincott Williams & Wilkins; 2004. p. 101-114.
8. Primm TP, Andersen SJ, Mizrahi V, Avarbock D, Rubin H, Barry CE 3rd. The stringent response of Mycobacterium tuberculosis is required for long-term survival. J Bacteriol 2000;182:4889–98. [PubMed: 10940033]
9. Artsimovitch I, Patlan V, Sekine S, et al. Structural basis for transcription regulation by alarmone ppGpp. Cell 2004;117:299–310. [PubMed: 15109491]
10. Perederina A, Svetlov V, Vassylyeva MN, et al. Regulation through the secondary channel--structural framework for ppGpp-DksA synergism during transcription. Cell 2004;118:297–309. [PubMed: 15294156]
11. Braeken K, Moris M, Daniels R, Vanderleyden J, Michiels J. New horizons for (p)ppGpp in bacterial and plant physiology. Trends Microbiol 2006;14:45–54. [PubMed: 16343907]
12. Manganelli R. Polyphosphate and stress response in mycobacteria. Mol Microbiol 2007;65:258–60. [PubMed: 17590232]
13. Potrykus K, Cashel M. (p)ppGpp: Still Magical? Annu Rev Microbiol. 2008
14. Avarbock D, Salem J, Li LS, Wang ZM, Rubin H. Cloning and characterization of a bifunctional RelA/SpoT homologue from Mycobacterium tuberculosis. Gene 1999;233:261–9. [PubMed: 10375643]
15. Avarbock A, Avarbock D, Teh JS, Buckstein M, Wang ZM, Rubin H. Functional regulation of the opposing (p)ppGpp synthetase/hydrolase activities of RelMtb from Mycobacterium tuberculosis. Biochemistry 2005;44:9913–23. [PubMed: 16026164]
16. Dahl JL, Kraus CN, Boshoff HI, et al. The role of RelMtb-mediated adaptation to stationary phase in long-term persistence of Mycobacterium tuberculosis in mice. Proc Natl Acad Sci U S A 2003;100:10026–31. [PubMed: 12897239]
17. Karakousis PC, Yoshimatsu T, Lamichhane G, et al. Dormancy phenotype displayed by extracellular Mycobacterium tuberculosis within artificial granulomas in mice. J Exp Med 2004;200:647–57. [PubMed: 15353557]
18. Flynn, J.; Chan, J. Animal models of tuberculosis. In: Rom, W.; Garay, S., editors. Tuberculosis. 2nd. Philadelphia: Lippincott Williams & Wilkins; 2004. p. 237-250.
19. McMurray DN. Disease model: pulmonary tuberculosis. Trends Mol Med 2001;7:135–7. [PubMed: 11286786]
20. Vandiviere HM, Loring WE, Melvin I, Willis S. The treated pulmonary lesion and its tubercle bacillus. II. The death and resurrection. Am J Med Sci 1956;232:30–7. passim. [PubMed: 13326887]
21. Via LE, Lin PL, Ray SM, et al. Tuberculous granulomas are hypoxic in guinea pigs, rabbits, and nonhuman primates. Infect Immun 2008;76:2333–40. [PubMed: 18347040]
22. Lenaerts AJ, Hoff D, Aly S, et al. Location of persisting mycobacteria in a Guinea pig model of tuberculosis revealed by r207910. Antimicrob Agents Chemother 2007;51:3338–45. [PubMed: 17517834]
23. Tsai MC, Chakravarty S, Zhu G, et al. Characterization of the tuberculous granuloma in murine and human lungs: cellular composition and relative tissue oxygen tension. Cell Microbiol 2006;8:218–32. [PubMed: 16441433]
24. Aly S, Wagner K, Keller C, et al. Oxygen status of lung granulomas in Mycobacterium tuberculosis-infected mice. J Pathol 2006;210:298–305. [PubMed: 17001607]
25. Ausubel, FM. Current protocols in molecular biology. New York: Greene Pub Associates and Wiley-Interscience: J. Wiley; 1991.
26. Sureka K, Dey S, Datta P, et al. Polyphosphate kinase is involved in stress-induced mprAB-sigE-rel signalling in mycobacteria. Mol Microbiol 2007;65:261–76. [PubMed: 17630969]
27. Lee MH, Pascopella L, Jacobs WR Jr, Hatfull GF. Site-specific integration of mycobacteriophage L5: integration-proficient vectors for Mycobacterium smegmatis, Mycobacterium tuberculosis, and bacille Calmette-Guerin. Proc Natl Acad Sci U S A 1991;88:3111–5. [PubMed: 1901654]

28. Jacobs WR Jr, Kalpana GV, Cirillo JD, et al. Genetic systems for mycobacteria. Methods Enzymol 1991;204:537–55. [PubMed: 1658570]
29. Allen SS, McMurray DN. Coordinate cytokine gene expression in vivo following induction of tuberculous pleurisy in guinea pigs. Infect Immun 2003;71:4271–7. [PubMed: 12874302]
30. Cho H, Lasco TM, Allen SS, Yoshimura T, McMurray DN. Recombinant guinea pig tumor necrosis factor alpha stimulates the expression of interleukin-12 and the inhibition of Mycobacterium tuberculosis growth in macrophages. Infect Immun 2005;73:1367–76. [PubMed: 15731034]
31. Lyons MJ, Yoshimura T, McMurray DN. Interleukin (IL)-8 (CXCL8) induces cytokine expression and superoxide formation by guinea pig neutrophils infected with Mycobacterium tuberculosis. Tuberculosis (Edinb) 2004;84:283–92. [PubMed: 15207803]
32. Skwor TA, Cho H, Cassidy C, Yoshimura T, McMurray DN. Recombinant guinea pig CCL5 (RANTES) differentially modulates cytokine production in alveolar and peritoneal macrophages. J Leukoc Biol 2004;76:1229–39. [PubMed: 15377675]
33. Converse PJ, Karakousis PC, Klinkenberg LG, et al. Role of the dosR-dosS two-component regulatory system in Mycobacterium tuberculosis virulence in three animal models. Infect Immun 2009;77:1230–7. [PubMed: 19103767]
34. Dahl JL, Kraus CN, Boshoff HI, et al. The role of RelMtb-mediated adaptation to stationary phase in long-term persistence of Mycobacterium tuberculosis in mice. Proc Natl Acad Sci U S A 2003;100:10026–10031. [PubMed: 12897239]
35. Jain SK, Hernandez-Abanto SM, Cheng QJ, et al. Accelerated detection of Mycobacterium tuberculosis genes essential for bacterial survival in guinea pigs, compared with mice. J Infect Dis 2007;195:1634–42. [PubMed: 17471433]
36. Klinkenberg LG, Sutherland LA, Bishai WR, Karakousis PC. Metronidazole lacks activity against Mycobacterium tuberculosis in an in vivo hypoxic granuloma model of latency. J Infect Dis 2008;198:275–83. [PubMed: 18491971]
37. Brennan MJ, Delogu G, Chen Y, et al. Evidence that mycobacterial PE_PGRS proteins are cell surface constituents that influence interactions with other cells. Infect Immun 2001;69:7326–33. [PubMed: 11705904]
38. Ramakrishnan L, Federspiel NA, Falkow S. Granuloma-specific expression of Mycobacterium virulence proteins from the glycine-rich PE-PGRS family. Science 2000;288:1436–9. [PubMed: 10827956]
39. Ly LH, McMurray DN. The Yin-Yang of TNFalpha in the guinea pig model of tuberculosis. Indian J Exp Biol 2009;47:432–9. [PubMed: 19634707]
40. Huygen K, Abramowicz D, Vandenbussche P, et al. Spleen cell cytokine secretion in Mycobacterium bovis BCG-infected mice. Infect Immun 1992;60:2880–6. [PubMed: 1612754]
41. Huygen K, Van Vooren JP, Turneer M, Bosmans R, Dierckx P, De Bruyn J. Specific lymphoproliferation, gamma interferon production, and serum immunoglobulin G directed against a purified 32 kDa mycobacterial protein antigen (P32) in patients with active tuberculosis. Scand J Immunol 1988;27:187–94. [PubMed: 3124263]
42. Post FA, Manca C, Neyrolles O, Ryffel B, Young DB, Kaplan G. Mycobacterium tuberculosis 19-kilodalton lipoprotein inhibits Mycobacterium smegmatis-induced cytokine production by human macrophages in vitro. Infect Immun 2001;69:1433–9. [PubMed: 11179309]
43. Wards BJ, de Lisle GW, Collins DM. An esat6 knockout mutant of Mycobacterium bovis produced by homologous recombination will contribute to the development of a live tuberculosis vaccine. Tuber Lung Dis 2000;80:185–9. [PubMed: 11052907]
44. Ly LH, Russell MI, McMurray DN. Cytokine profiles in primary and secondary pulmonary granulomas of Guinea pigs with tuberculosis. Am J Respir Cell Mol Biol 2008;38:455–62. [PubMed: 18032570]

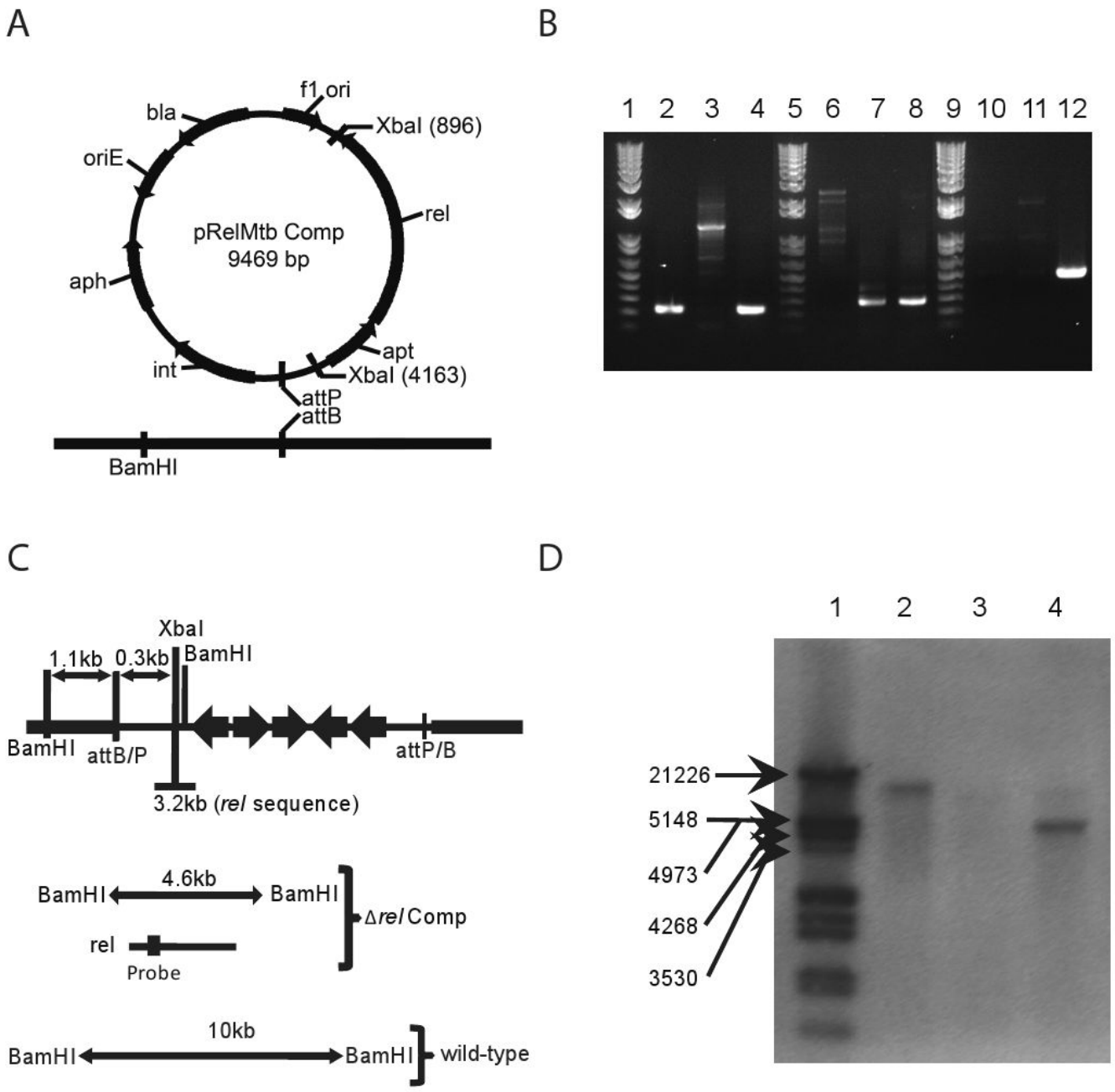

Figure 1.

Complementation of Δ*rel*. A. Diagram of expected recombination between integrating plasmid and genomic DNA. B. PCR analysis of genomic DNA. Lanes 2-4 show the presence of *rel* in wild-type and *rel* Comp strains. Lanes 6-8 show the presence of a region of the hygromycin gene marking the deletion of *rel* in both the Δ*rel* and *rel* Comp strains. Lanes 10-12 show the presence of a region of the kanamycin gene marking the complementation of *rel* in only the *rel* Comp strain. C. Diagram of expected sizes of genomic gene fragments expected to bind to probe recognizing region of *rel* coding sequence. D. Southern blot showing *rel* as a single copy gene present in the correct fragment size in both wild-type and *rel* Comp strains.

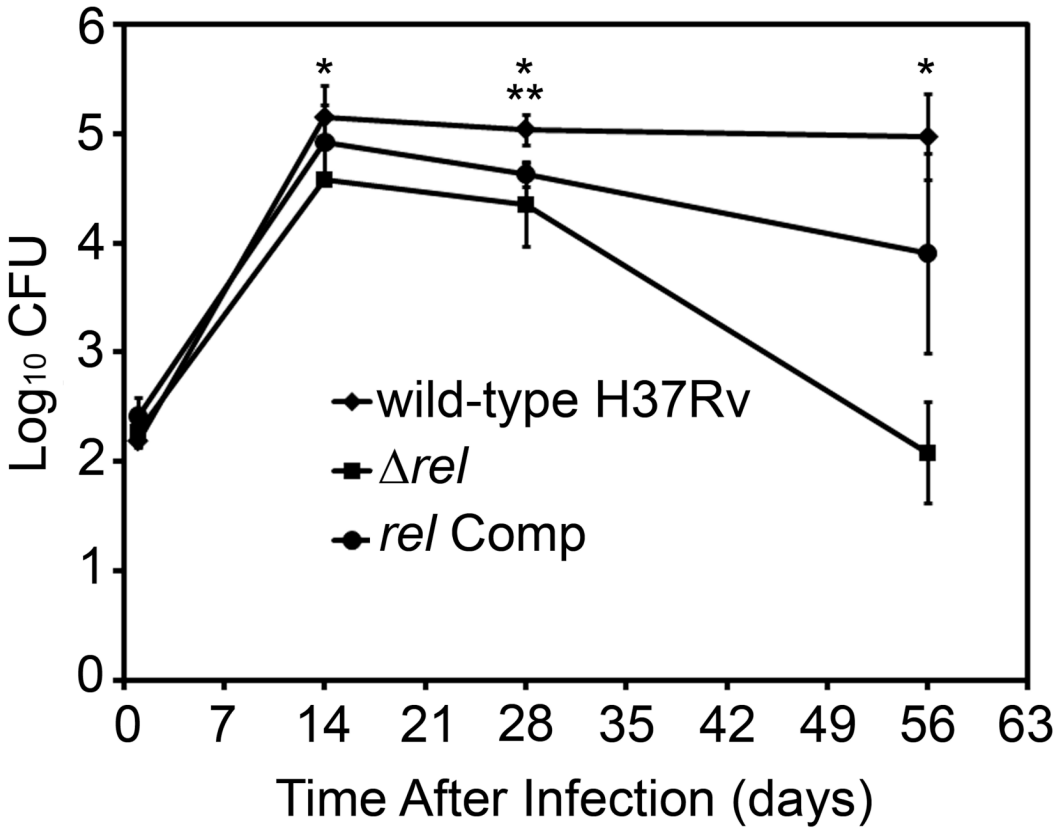

Figure 2.
Reduced initial growth and survival of Δ*rel* strain in the lungs of guinea pigs after low-dose aerosol infection. CFU = colony-forming units. * indicates significant differences between CFU recovered from wild-type and mutant infected lungs (p<=.01). ** indicates the only time point with a significant difference between the wild-type group and the *rel* Comp group (p=0.004).

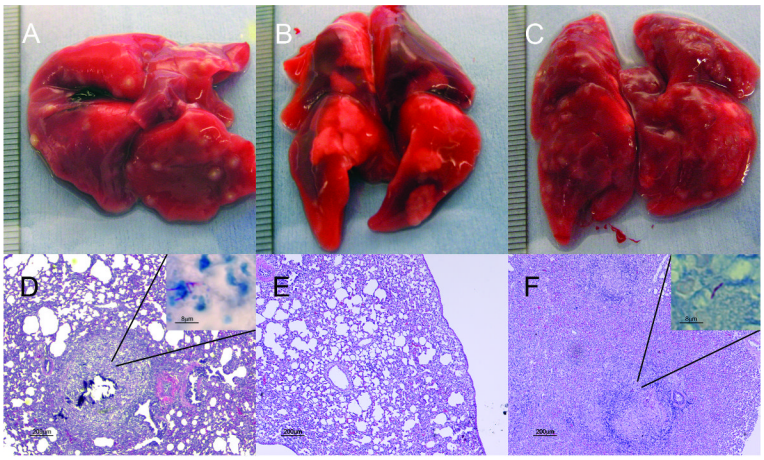

Figure 3.

Guinea pig lung pathology after 56 days of infection with *Mycobacterium tuberculosis.* Gross pathology (A-C) and histology (D-F) of lung samples from animals infected with H37Rv (A, D), H37Rv Δ*rel* (B, E), or H37Rv Δ*rel* Comp (C, F). Ziehl-Neelsen stain demonstrating the presence of acid-fast bacilli in the periphery of lung granulomas of animals infected with H37Rv (D inset) and Δ*rel* Comp (F inset). Acid-fast bacilli were not detectable in lung granulomas of Δ*rel*-infected animals (E).

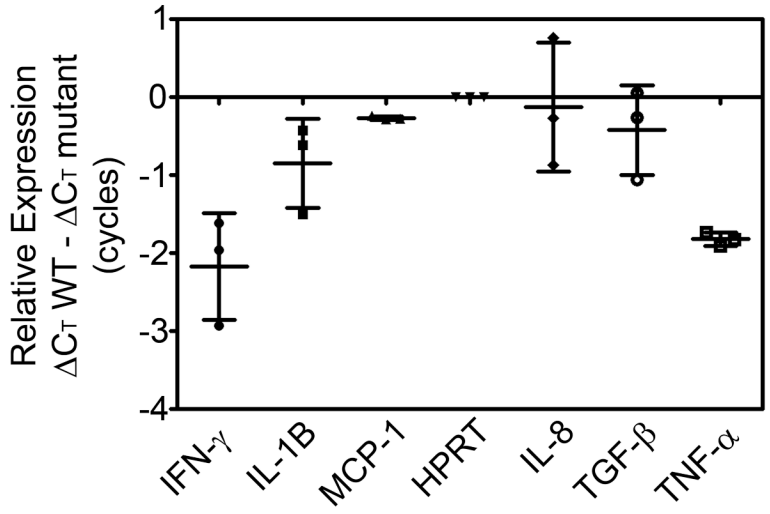

Figure 4.

Similar relative abundance of mRNA transcripts from guinea pig lungs following 28 days of infection with Δ*rel* strain compared to wild-type. Data points indicate values from individual Δ*rel*-infected animals. Error bars represent standard deviation. mutant = Δ*rel* strain; WT = wild type (H37Rv) strain; ΔC_T = cycle threshold (C_T) on Day 28 – C_T on Day 1. IFN-γ (p=.06), IL-1B (p=.20), MCP (p=.11), IL-8 (p=.88), TGF-β (p=.47), and TNF-α (p=.003).

Table 1

Assessment of additional virulence parameters in the guinea pig

Day 1		**Body Weight (g)**	**Lung Weight (g)**	**Spleen Weight (mg)**	**Spleen CFU (log_{10})**
	WT H37Rv	263.50 ± 57.04	ND	313 ± 76	ND
	Δ*rel*	290.20 ± 24.94	ND	420 ± 134	ND
	rel Comp	273.90 ± 16.49	ND	470 ± 158	ND
Day 28					
	WT H37Rv	532.85 ± 29.50	5.13 ± 0.38	1233 ± 217	3.53 ± 0.80
	Δ*rel*	524.60 ± 37.06	4.47 ± 0.27	895 ± 159	2.75 ± 0.82
	rel Comp	563.13 ± 28.53	3.84 ± 0.25	1110 ± 245	3.47 ± 1.23
Day 56					
	WT H37Rv	714.33 ± 34.34	5.26 ± 0.21	873 ± 84	2.10 ± 1.28
	Δ*rel*	640.78 ± 120.84	4.22 ± 0.81	648 ± 161	1.56 ± 1.02
	rel Comp	710.23 ± 24.83	5.06 ± 0.43	955± 145	2.98 ± 0.71

NOTE. Data are mean colony-forming units (CFU) ± standard deviation. ND = Not determined.